Available online at www.sciencedirect.com

ScienceDirect

Energy Procedia 94 (2016) 3 – 19

Energy Procedia

13th Deep Sea Offshore Wind R&D Conference, EERA DeepWind'2016, 20-22 January 2016, Trondheim, Norway

Validation of a FAST Model of the Statoil-Hywind Demo Floating Wind Turbine

Frederick Driscoll[a]*, Jason Jonkman[a], Amy Robertson[a], Senu Sirnivas[a], Bjørn Skaare[b], Finn Gunnar Nielsen[b]

[a]*National Renewable Energy Laboratory, 15013 Denver West Parkway, Golden, CO 80401, United States of America*
[b]*Statoil ASA, Sandsliveien 90, Bergen, N-5020, Norway*

Abstract

To assess the accuracy of the National Renewable Energy Laboratory's (NREL's) FAST simulation tool for modeling the coupled response of floating offshore wind turbines under realistic open-ocean conditions, NREL developed a FAST model of the Statoil Hywind Demo floating offshore wind turbine, and validated simulation results against field measurements. Field data were provided by Statoil, which conducted a comprehensive test measurement campaign of its demonstration system, a 2.3-MW Siemens turbine mounted on a spar substructure deployed about 10 km off the island of Karmøy in Norway. A top-down approach was used to develop the FAST model, starting with modeling the blades and working down to the mooring system. Design data provided by Siemens and Statoil were used to specify the structural, aerodynamic, and dynamic properties. Measured wind speeds and wave spectra were used to develop the wind and wave conditions used in the model. The overall system performance and behavior were validated for eight sets of field measurements that span a wide range of operating conditions. The simulated controller response accurately reproduced the measured blade pitch and power. The structural and blade loads and spectra of platform motion agree well with the measured data.

Peer-review under responsibility of SINTEF Energi AS

Keywords: FAST; model validation; StatoilHywind demo; floating offshore wind turbine; measurement data; open-ocean conditions

* Corresponding author. Tel.: +1-303-384-7153; fax: +1-303-384-7003.
E-mail address: frederick.driscoll@nrel.gov

Peer-review under responsibility of SINTEF Energi AS
doi:10.1016/j.egypro.2016.09.181

1. Introduction

Offshore wind energy development is pushing into deeper water to harness the vast wind resources that lie further offshore. As water depth increases beyond 50-60 m, unfavorable structural characteristics along with increasing foundation and installation costs render fixed-bottom wind substructures uneconomic [1,2]. Floating platforms are being considered as less expensive alternatives because the costly substructure of a fixed platform is replaced by mooring lines and a floating substructure. These new platforms depart from conventional land-based and fixed-platform experience and design methods because floating platforms are not constrained by the nearly rigid connection to the sea floor that hold fixed-bottom structures in place. The flexible mooring lines used for station keeping allow six degree-of-freedom platform motion (surge, sway, heave, roll, pitch and yaw). For floating spar buoys, roll and pitch restoring moments are provided by a buoyancy-weight couple (the center of gravity is much lower than the center of buoyancy) and the mooring lines provide the translational restoring force and the yaw restoring moment.

The coupled nonlinear interaction between aerodynamic, hydrodynamic, and structural forces with the turbine control makes design of floating wind platforms challenging. Several analysis approaches exist for modeling the interactions, from uncoupled linear spectral fatigue models to coupled nonlinear time-domain simulations. While uncoupled models are attractive because of their simplicity, offshore wind designs have tight margins and reducing uncertainty is essential to keeping safety factors and costs low. Coupled modeling is needed to capture important system aero-hydro-servo-elastic interactions. Coupled models can reduce design uncertainty by modeling the entire offshore structure (from the turbine down to the foundation) within one tool, while concurrently accounting for loads, dynamics, and control. Coupled modeling is therefore used for design and structural optimization. Coupled modeling is also required in the draft International Electrotechnical Commission (IEC) 61400-3-2 design technical specification for floating offshore wind systems.

FAST [3], developed at the U.S. Department of Energy's (DOE) National Renewable Energy Laboratory (NREL), is a coupled multi-physics engineering tool that can model wind and wave inflow fields; rotor aerodynamics; platform and mooring hydrostatics/dynamics; structural dynamics of the blades, drivetrain, tower and substructure; and controls of offshore wind turbines.

For coupled models, verification against other models and validation against experimental data are needed to understand limits and accuracy. Validation can also highlight deficiencies in the modeling tools and approaches and help identify areas needed for model tool improvement. The turbine and tower modeling capabilities of FAST have been extensively validated using data from onshore wind turbines. FAST has been verified against several other floating offshore wind tools in the International Energy Agency (IEA) Wind Task 23 Offshore Code Comparison Collaboration (OC3) and Wind Task 30 OC3 Continued (OC4) projects [5,6]. Validation of the floating wind turbine modeling capability of FAST has been done using scale-model data from testing performed by the DeepCwind consortium on three different floating structures in the Maritime Research Institute Netherlands' wave basin [7]. Limited validation has been performed against open-ocean measurements for the SWAY [8] and WindFloat[†] systems. Further validation against field data for a megawatt-scale floating wind turbine is needed.

In this paper, FAST is validated using a comprehensive set of field measurements from Statoil's Hywind Demo, a spar-mounted, floating offshore wind turbine. Data were provided by Statoil for 8 operating cases with wind speeds that span the wind turbine operating range from about 4 to 25 m/s. Prior to validation, the model response was calibrated so the natural periods of motion obtained from simulated free-decay tests agreed within a few percent of the measured values. The mean power curve was verified for wind speeds that span the operational range from 0 to 25 m/s. Validation was performed for 1) the controller, 2) the rotor blades, and 3) the platform motion. Most data presented in this paper is either normalized or without units so as to protect proprietary information.

[†] The results of the WindFloat validation are not publicly available.

2. Model description

Hywind is a floating spar offshore wind turbine developed by Statoil. The Hywind Demo is a demonstration system that was installed and commissioned in Norway in 2009; it was the world's first full-scale floating offshore wind turbine. The installed capacity of the demo system is 2.3 MW. The demo unit is located 10-km west of the island of Karmøy off the Norwegian west coast. The water depth is 220 m. This demonstration project proved that the Hywind floating substructure is a suitable platform for conventional multi-megawatt turbines.

Fig. 1. Statoil's Hywind Demo floating offshore wind turbine utilizing a Siemens' 2.3-MW Turbine with an 82.4-m rotor diameter.

The Hywind concept consists of a spar platform that supports a Siemens 2.3-MW wind turbine with a rotor diameter of 82.4 m. The spar is a slender cylindrical structure that extends 100-m below the surface with a diameter of about 8.3 m [9,10]. The spar limits wave-induced movements and loading to the structure by reducing the cross-sectional area in the splash zone, while at the same time reducing the substructure cost. The structure is ballast-stabilized and attached to the seabed by three separate catenary mooring lines. At the sea floor, the three mooring lines are attached to anchors. Near the surface, the mooring line splits into a bridle attachment that connects to the hull, increasing the yaw stiffness. The mooring system has inherent design redundancy. Large clump weights are attached to each mooring line close to the mid-span of the mooring. Hywind Demo uses a proprietary variable speed, collective blade-pitch controller that stabilizes platform-pitch motion [11].

2.1. Simulation

The simulation of the Hywind Demo floating turbine is performed using FAST v7‡ [3]. During simulation, wind turbine aerodynamic and structural response to wind-inflow conditions and the hydrodynamic response of the platform to incident waves are determined nonlinearly in time. FAST also integrates active generator and blade-pitch controls so that turbine power regulation and motion mitigation are included. Output from the simulation includes time series of loads, motions, and structural deflections.

The system model consists of the following primary components: 1) three rotor blades; 2) the hub, nacelle, driveshaft, and generator; 3) the tower; 4) the substructure; and 5) the mooring system. The rotor blades, driveshaft, tower, and mooring lines are modeled as flexible structural members, while the hub, nacelle, generator, and substructure are rigid.

The turbine structural data and airfoil data were provided by Siemens and the platform inertial properties, mooring layout, and controller were provided by Statoil. The following data were assimilated into FAST:

- Airfoil lift and drag curves (two-dimensional), mass, and structural-elastic properties at stations along the blades
- Inertia properties of the nacelle
- Inertia and structural-elastic properties of the drive train
- Mass and structural-elastic properties at stations along the tower, from the waterline to the tower top
- Mooring configuration and line properties
- Hydrodynamic coefficients of the spar
- Statoil's generator and pitch controller (provided as a black-box)
- Inertia properties of the rigid spar.

2.2. Blade/tower model

BModes [12], an NREL preprocessing finite-element tool that provides dynamically coupled modes for a beam, was used to calculate the blade (and tower) mode shapes in the flap (fore-aft) and edge (side-to-side) directions. These mode shapes were approximated with 6^{th}-order polynomials for use in FAST. For the blades, the coordinates of the elastic center at each cross section provided by Siemens follows a curve, distinct from the pitch axis of the blade. At the time of this study (although this limitation has now been addressed), FAST required that the pitch axis and elastic axis be coincident and straight. Therefore, it was necessary to best fit the FAST pitch axis to the Siemens elastic coordinate data. Similarly, the aerodynamic center of the Siemens blade model is defined as the ¼ chord point that can be offset from the pitch axis in two directions. In FAST, the aerodynamic center could only be located along the cord line, relative to the pitch axis. Therefore, a transform was applied to best approximate the FAST aerodynamic center relative to the Siemens data.

AirfoilPrep, another NREL preprocessor, was used to apply rotational augmentation corrections for three-dimensional delayed stall to the airfoil lift and drag curves.

2.3. Platform/mooring model

Statoil supplied the substructure and mooring geometry and gross system mass properties for the Hywind Demo. To ensure the modeled response of the spar was close to values specified by Statoil, the spar mass center and inertia characteristics were estimated by NREL. For the purposes of this estimate, the spar platform was assumed to be a single-compartment, single-wall design with a ring-stiffened column.

To employ a first-order potential-flow model for the hydrodynamic loads, FAST requires a linearized frequency-domain radiation and diffraction solution from WAMIT (a computer program based on potential theory) [4]. In WAMIT, the platform geometry was modeled to the water surface and a B-spline representation of the geometry

‡ This work was performed before the newer and more capable FAST v8 was available.

was used to generate hydrodynamic coefficient data sets (using the higher-order geometry method) for added mass and damping, diffraction exciting forces, and hydrostatic restoring forces. In addition to potential-flow, the FAST model includes viscous drag for transverse motions of the spar (for surge, sway, roll, and pitch motion, but not heave or yaw motion) through the relative-velocity form of the drag term from Morison's equation, as well as additional linear damping in surge, sway, heave, and yaw (outside of WAMIT, to mimic additional viscous effects) with coefficients derived in the OC3 program (despite the differences in geometry) [5].

As previously mentioned, a three-leg mooring system is used. Each line uses a bridle attachment to the spar and has a large clump weight suspended just above the ocean bottom. The mooring line also consists of dissimilar sections. At the time of this study (although this limitation has now been addressed), FAST used a quasi-static catenary mooring line with uniform properties and no line-to-line interconnections. As such, a mooring line representation was chosen that yields similar lateral stiffness and fairlead line loads; the equilibrium point was the same for the model and the real system. The yaw stiffness in FAST was augmented to match the total mooring yaw stiffness.

2.4. Wind/wave models

The wind-inflow data used were generated in TurbSim [13]. TurbSim is a full-field, turbulent-wind simulator that typically uses synthetic models (based on a prescribed wind spectrum and coherence functions) to generate time series of three-component wind-speed vectors at points in a two-dimensional grid across the rotor-swept area. However, TurbSim has recently been updated to derive the wind field in the grid based on one or more known time series at given points instead of a prescribed wind spectrum. This new feature was used to generate the wind field based on wind speed measurements from a nacelle-mounted anemometer on the Hywind Demo. The resulting time series match the measured data at the hub (grid center); TurbSim used the input wind-speed measurements to calculate velocity spectra and mean wind speed for the other points on the grid (assuming a power-law wind profile and IEC coherence functions).

Linear, first-order wave time histories were generated in FAST by discretizing a JONSWAP spectrum and summing the different frequencies of wave motion. The significant wave height, the peak wave period, and the spectral shape parameter were specified to best match the measured wave spectra.

2.5. Controller

The Hywind Demo utilizes a two-tiered controller. The base controller is provided by Siemens and is made for a conventional land-based wind turbine. Statoil employs an addition control loop that sits on top of the Siemens controller. The Statoil controller uses blade-pitch control to mitigate the motion of the floating platform. Statoil supplied NREL with a single-turbine controller as a black box that approximates the combined-control response of the combined Siemens-Statoil controller, and this controller was integrated into the FAST model.

2.6. Model differences

Although every attempt was made to accurately model and simulate the Hywind Demo, simplifications had to be made due to limits on data and modeling capabilities. Therefore, known differences between the simulation and Hywind Demo are listed:

- The turbine nacelle-yaw control is not included (fixed nacelle-yaw is modeled instead; platform-yaw is included).
- A unidirectional single peak wave field is modeled based on measured wave statistics, rather than using the actual time series.
- A uniform mooring line without a bridle attachment is used instead of the multi-segment line with the bridle. The effect of the clump weight is incorporated in the single-line model and yaw stiffness is augmented with a yaw spring.
- Blades are modeled as straight (no sweep) with the aerodynamic centers only varying along the blade chord.
- The controller used in the model is not identical to the one used by the real turbine.

3. Data

The Hywind Demo is equipped with more than 200 sensors to measure the environmental conditions and system response. Measurements used in this analysis include:

- Wind speed and direction at the nacelle via a sonic anemometer, not corrected for nacelle motions or rotor-wake effects
- Wave elevation time series via airgap sensors that measure the distance between the platform deck and the sea surface, corrected for platform motions and diffraction
- Average current profiles from a surface-mounted acoustic current profiler
- Motions in all six degrees of freedom at the waterline and in the nacelle via inertial measurement units and GPS
- Blade-root strains in the flap and edge directions
- Low-speed shaft torque
- Wind turbine control states that include blade pitch, rotor speed, power production, and nacelle-yaw angle; all via the turbine controller.

Statoil has been continuously recording measurements from these and other sensors since 2009, yielding a comprehensive set of data. For this analysis, Statoil provided NREL with eight data sets each with approximately stationary wind and wave conditions, Table 1. Time-series lengths are between 35 minutes and 1 hour. In all eight cases, the turbine is operating and producing power.

All mechanical load and moment data were provided in terms of strain. No scale factors and offsets were available to convert measurements into physical quantities, such as loads. To compare the force and moment measurements with model results, scale factors and offsets were chosen to fit measurements to model data. As such, a direct quantification of model uncertainty is not possible. Data are sufficient to provide a general level model validation.

Table 1. Overview of the environmental conditions for the eight data sets provided by Statoil.

Case no.	Duration (min)	Mean wind speed (m/s)	Wind direction (coming from) (deg)	Significant wave height (m)	Peak-spectral wave period (s)	Peak-shape parameter (-)	Wave propagation direction (deg)	Mean current speed (m/s)	Current direction (deg)	Turbine status
1	60	4.7	151	0.88	7.0	2.2	4	0.40	138	Producing power
2	60	9.1	36	1.3	6.9	1	144	0.31	68	Producing power
3	60	9.7	15	1.4	8.6	2	146	0.32	316	Producing power
4	35	12.8	227	3.3	9.7	1.1	25	0.29	50	Producing power
5	35	13.4	252	5.2	10.3	1.74	79	0.52	89	Producing power
6	35	17.5	147	4.0	10.0	1.2	355	0.43	337	Producing power
7	35	18.3	165	2.0	6.8	2.2	353	0.38	316	Producing power
8	35	21.7	152	2.3	7.1	2	358	0.30	336	Producing power

4. Model calibration and verification

4.1. Calibration

Model calibration was performed to tune the spar motions to match measured values by slightly adjusting model variables where uncertainty exists. First, the mass distribution of the blade was increased by 0.46% and the tower

mass distribution was increased by 3.6% so the gross mass of these components matched those specified by Statoil. Otherwise, the structural properties of the blades and tower remain as specified and the aerodynamic properties of the blades are also not changed beyond the simplifications assumed in the model development.

The natural periods of the platform motion are provided in [9,10] and were estimated from power spectra of the field measurements (Table 2). During the model calibration process, free-decay simulations were used to calculate the natural periods of the platform motion predicted by the FAST model. As previously mentioned, the FAST model used simple catenary mooring lines with uniform properties and no line-to-line interconnections. Therefore, the surge and sway modes were tuned by slightly adjusting mooring line mass and length. The spar center of gravity was estimated by NREL, and uncertainty exists in this estimate; therefore, the roll and pitch natural periods were tuned by adjusting the vertical location of the center of mass. The yaw response was adjusted by tuning the yaw-stiffness term. After tuning, the natural periods agreed well in all degrees of freedom. Damping was not calibrated because of the lack of suitable measurement data.

Table 2. Comparison of the measured natural periods of the spar motion with values from the tuned model.

	Measured (s)	Simulated (s)
Surge	125.0	120.0
Sway	125.0	119.5
Heave	27.5	27.8
Roll	23.9	25.6
Pitch	23.9	25.1
Yaw	6.2	7.36

4.2. Verification

FAST has been extensively verified against other models of floating offshore wind turbines in the IEA Wind Task 23 and 30 OC3 and OC4 projects. However, case-by-case verification is still needed to ensure a particular model's response characteristics are accurate. For the Hywind Demo model, verification was performed to confirm that the model physically represents the real system and to identify differences that may cause uncertainty in the model results and validation. Model-calculated values for the geometry, mass, inertia, and structural natural frequencies were first compared with values provided by Siemens and Statoil. The mass properties and first modal frequency of the blades (nonrotating) and towers (with fixed base) matched those specified (Table 3 and Table 4). Because the blade and tower mass properties were individually tuned, the aggregate masses are within 1% of the specified values. The first model frequencies of the blades agree to the specified values to within 1 %; however, the second mode frequencies were off by 3.5% and 4.1% in the flap and edge directions, respectively. The first tower mode was off by nearly 9%, but the second mode agreed to within 1%. The modes were not tuned.

Table 3. Comparison of the normalized mass properties calculated by FAST versus those specified.

	Specified	Calculated by FAST
Blade mass	1	1
Blade CoG	1	1.007
Second mass moment	1	0.9954
Tower-top mass	1	1.0002
Tower mass	1	0.993

Table 4. Comparison of the normalized model frequencies of the rotor blades (nonrotating) and tower as calculated by BModes versus those specified.

	Specified	Calculated by BModes
Flap blade mode 1	1	1.008
Flap blade mode 2	1	1.03
Edge blade mode 1	1	1.006
Edge blade mode 2	1	1.04
Tower mode 1	1	0.91

Tower mode 2	1	0.99

To ensure the power curve and the rotor speed predicted by the FAST model is accurate, several simulations were run with different constant wind speeds ranging from 0 to 25 m/s. Simulations were performed with the spar rigidly fixed in the inertial frame and with the spar able to move in six degrees of freedom (without waves), but using the mooring for station-keeping to identify any impact on power production from the floating system. The power is presented for the steady system, once all transients died out, and compared to the Siemens-supplied power curve in Fig. 2. Note that the Siemens power curve was produced with simulations internal to Siemens using different turbulence and shear conditions. Therefore, this curve is not the sales power curve and no inference to the manufacturer's specified performance can be made.

The generator power at wind speeds below 10 m/s and above 15 m/s agree well with the power curve provided by Siemens. However, near rated wind speed, the FAST model slightly over-predicts the power as the controller transitions between region 2 and 3, likely due to the approximated controller provided by Statoil. The theoretical rotor speed curve was not provided. Qualitatively, the rotor speed, the lower plot in Fig. 2, behaves as expected. The floating foundation does not have a negative impact on the performance under the conditions simulated here.

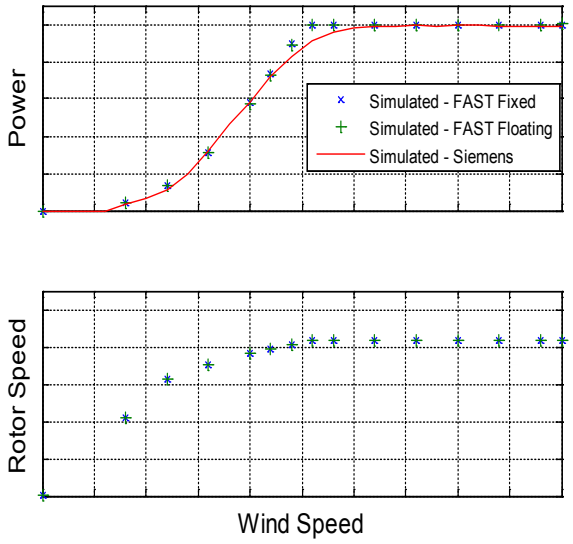

Fig. 2. Comparison of the power curve calculated by the model with the spar fixed and floating against the Siemens-specified power curve. The simulated rotor speed as a function of wind speed is also shown. Note: the Siemens power curve was produced from an internal model using different turbulence and shear conditions.

5. Validation

Validation of the FAST model is performed for the controller, the blade and rotor response, and the spar motion response.

To validate the turbine response against experimental data, the environmental conditions used in the simulation must closely match those specified in Table 1. In particular, to compare the measured and simulated response spectra, the wind and wave input must have the same energy distribution as that experienced by the Hywind Demo platform during measurement.

Time series of the wind speed measured by a sonic anemometer at the nacelle were used to generate the wind inflow. Wind speeds measurements in three directions at a single point, approximately hub height, were used to derive the full wind field across the rotor using TurbSim. The calculated wind speed time series at hub height, and centered with the rotor, closely matches the time series measured by the nacelle anemometer. It should be noted that

the sonic anemometer is behind the rotor and subject to a rotor-wake-induced velocity deficit and increased turbulence. The simulated signal closely follows the measured signal, but uses an IEC coherence function to derive the flow field across the rotor disk.

At the time of this study (although this limitation has now been addressed), the wave elevation and water particle motion used in the FAST simulation could only be calculated using a unidirectional JONSWAP spectrum, not the measured wave spectrum or the measured time series. Thus, for each measurement case, the significant wave height, wave peak-spectral period, and peak shape parameter of the JONSWAP spectrum were set to match those measured. Similarly, the wave direction of travel was set to the measured mean value. It should be highlighted here that any multidirectional and multimodal characteristics that may have occurred during the measurement campaign are not modeled here.

5.1. Control

The Hywind Demo controller manages not only the generator torque, rotor rpm, and blade pitch, but it also mitigates the platform pitch. Thus, prior to validating any response, the controller must first be validated. Because the wind speed measured at the nacelle is used in TurbSim to develop the inflow wind field and because the nacelle motion is more driven by wind than waves, the time series of the measured and simulated blade pitch can be directly compared (Fig. 3 and Fig. 4). The blade pitch response of the simulated controller tracks the measured pitch well at low frequencies. Matching the low-frequency blade-pitch response is important for the Hywind Demo because it is used to control the platform pitch. As expected, the blade pitch is fixed until rated power is reached, after which the pitch increases with wind speed. Throughout the wind speed range, the five-minute average rotor pitch closely agrees with measured valued. The model controller exhibits higher frequency content.

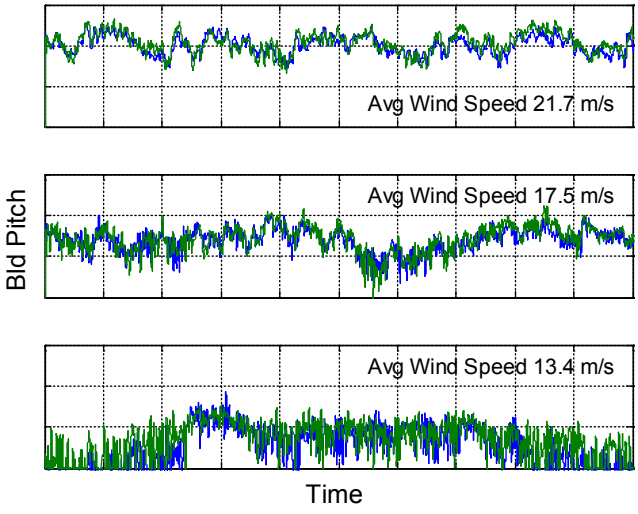

Fig. 3. Time series of the measured (blue) and simulated (green) blade pitch for three different average wind speeds, 21.7, 17.5, and 13.4 m/s.

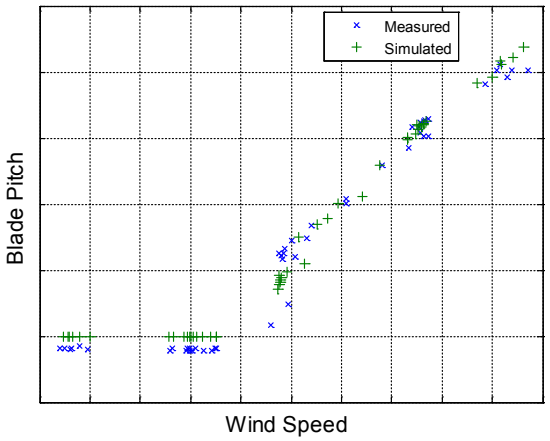

Fig. 4. Five-minute averages of the measured (blue) and simulated (green) blade pitch for all eight cases.

The torsional strain in the low-speed shaft was measured, but no scale factors were provided to convert strain to torque. Therefore, a scale factor and offset (to remove signal bias) were chosen to fit the measured torque with the modeled values. The power provides a reference to scale the torque because the rotor speeds are nearly identical. The scale factor and offset were derived from a subset of the results and applied to all results. The measured and modeled torques agreed well, with the model slightly over-estimating the torque below rated power (Fig. 5). The torque follows the expected trend, with torque increasing through region 2 and after rated power is reached, in region 3, the torque is held constant. For this work, the turbine is performing as expected and the slight over-predictions of power and torque by the model in region 2 are likely caused by simplifications in the blade model, the use of an approximate controller, and the use of the nacelle-based wind measurements. For example, the wind shear, wind veer, and turbulence levels for the measured response are unknown. Therefore, calculation of the measured power curve is not IEC compliant and no inference can be made about actual turbine performance.

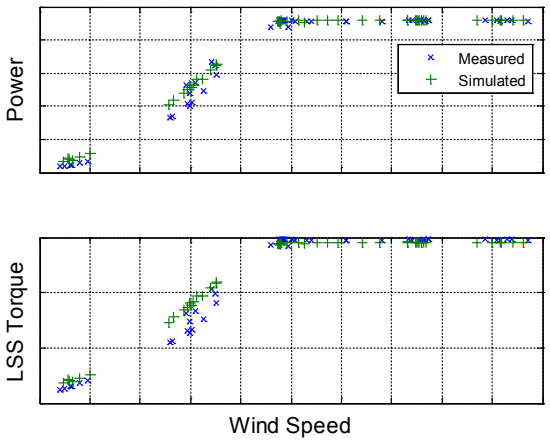

Fig. 5. Five-minute averages of the measured (blue) and simulated (green) generator power and low-speed shaft torque for all eight cases. Note: because of different controllers, simplifications in the model geometry, and the fact that inflow conditions were measured at a single point behind the rotor (freestream wind shear, wind veer, and turbulence are unknown for the measured response), no inference on turbine performance can be made.

5.2. Blade and rotor response

Edge and flap strains were measured at the blade root. Similar to the rotor torque, no scaling factors were provided to calculate moments. Therefore, a scale factor and offset were estimated so the measured and simulated five-minute average variance and mean agree. (The scale factor and offset were derived from a subset of the results and applied to all results.) As such, only comparison of the general response can be made; direct comparisons of signal magnitude cannot be made.

For use in design, models must accurately predict both mean load and load variance. Five-minute averages of the blade moments are presented in Fig. 6, and variances of the blade moments are presented in Fig. 7. The flap moments agree over the full range of wind speeds. As the wind speed increases up to rated power, the flap moments increase accordingly. After rated power is reached, the blades are pitched to maintain torque and the mean flap moments decrease with increasing wind speed. The variance of the flap moment agrees well and increases with wind speed. The modeled variance of the flap moment is slightly conservative.

The trend of the 5-minute average mean edge moment agrees over the wind speeds and in magnitude up until rated power. After that, the measured moment is somewhat larger than the simulated value. The flap moment is much larger than the edge moment and this difference in the edge moment may be due to a slight misalignment of the strain gages from the principle edge and flap axes. The variance of the edge moment is highest at lower wind speeds where the gravity signal is dominant. At higher wind speeds, the blades are pitched and wind loads have greater effect on the moments. Overall, the measured and simulated variance follow the same trend, with the simulated flapwise variance being slightly more conservative at higher wind speeds and slightly less conservative at lower wind speeds.

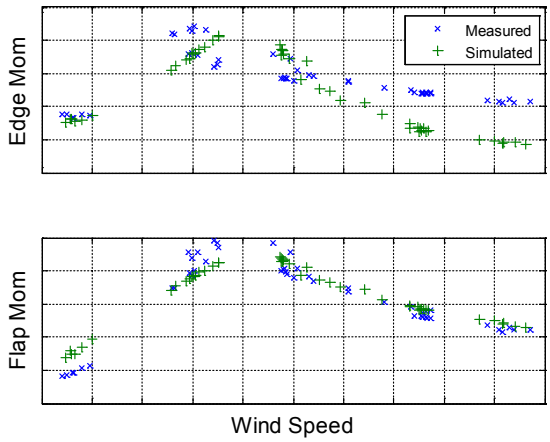

Fig. 6. Five-minute averages of the measured (blue) and simulated (green) rotor blade edge (upper plot) and flap (lower plot) moments.

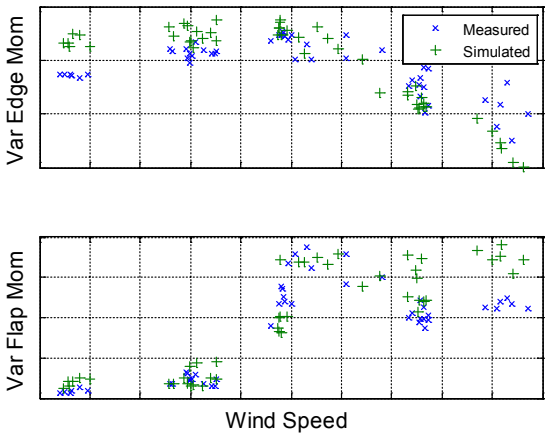

Fig. 7. Five-minute average variances of the measured (blue) and simulated (green) rotor blade edge (upper plot) and flap (lower plot) moments.

5.3. Spar motion

Access to data from the Statoil field campaign offers a unique opportunity to evaluate FAST's ability to simulate the motions of a spar-mounted turbine while operating in realistic open-ocean conditions. Statoil provided measurements of the spar in all six degrees of freedom. These measurements are referenced to an earth-fixed reference frame where the *X*-axis points northward, the *Y*-axis points west, and the *Z*-axis points upward. The origin is at the mean sea surface in the center of the spar. Rotation angles are specified clockwise when looking down the axes from the origin. These motion data were rotated into the FAST reference frame where surge is positive downwind, sway is positive to the left when looking downwind, and heave is positive upwards. Roll is defined as rotation about the surge axis, pitch as the rotation about the sway axis, and yaw as the rotation about the heave axis. The translation measurements were filtered by the data acquisition system to eliminate motion with periods longer than 30 s; thus, the natural periods of translation cannot be evaluated.

For brevity, only the following two cases are presented:

- Case 6: H_s = 1.4 m, T_p = 8.6 s , and W_s = 9.7 m/s
- Case 1: H_s = 4.0 m, T_p = 10.0 s, and W_s = 17.5 m/s

where H_s is the significant wave height, T_p is the peak-spectral period of the wave and W_s is the mean wind speed. The cases were selected to span a range of wave conditions, but also were a good match between the measured and model wave spectrum (Fig. 8). (The modelled wave spectrum is not smooth because of the use of randomized amplitudes.) For the first case, H_s = 1.4 m, the turbine is operating in region 2, whereas in the second case, H_s = 4.0 m, the turbine is operating in region 3.

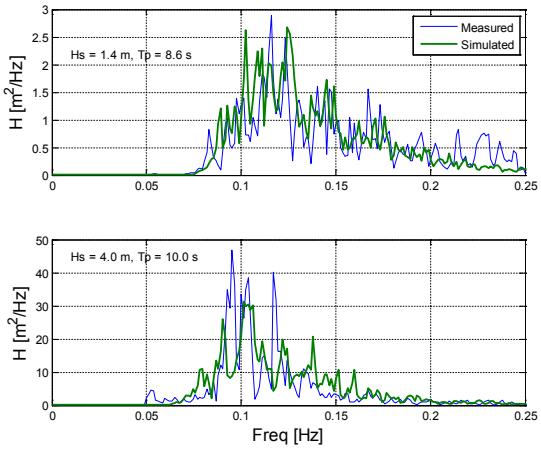

Fig. 8. Comparison of the measured (blue) and simulated (green) wave spectra.

In the wave band, from 0.06 to 0.25 Hz, the spectra of the measured and simulated translational motion (Fig. 9 and Fig. 12) closely agree over all wave frequencies. For the high significant wave height, H_s = 4.0 m, the simulated response at lower frequencies is slightly higher than measured in surge, sway, and heave. Similarly, within the wave band, the spectra of the roll and pitch agree in both cases (Fig. 10 and Fig. 13). As in the spectra of the translational motion for the high significant wave height, H_s = 4.0 m, the model over-predicts the response at lower frequencies between 0.06 and 0.08 Hz. At even lower frequencies, the natural period of roll and pitch can be seen around 0.04 Hz (Fig. 11 and Fig. 14). The higher excitation of the measured roll may be caused by spread seas, not modeled. As expected, the measured and predicted yaw response are somewhat different, and this is likely because of 1) the simplified mooring model used – the model does not include the bridle attachment to enhance the yaw stiffness, 2) the real waves are not unidirectional as in the model, 3) turbine yaw is fixed in the model and 4) The turbulent wind-inflow variation across the rotor is unknown, so, likely modeled differently.

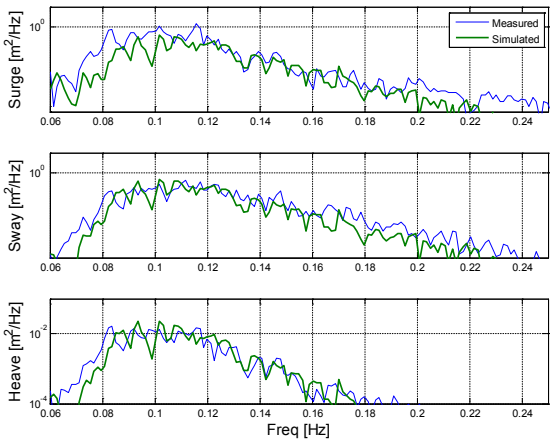

Fig. 9. Spectra of the translational motions of the spar in the wave-frequency range for H_s = 1.4 m, T_p = 8.6 s.

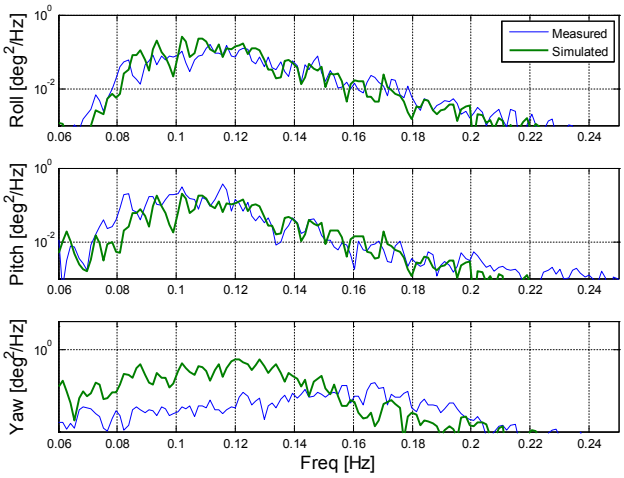

Fig. 10. Spectra of the rotational motions of the spar in the wave-frequency range for H_s = 1.4 m, T_p = 8.6 s.

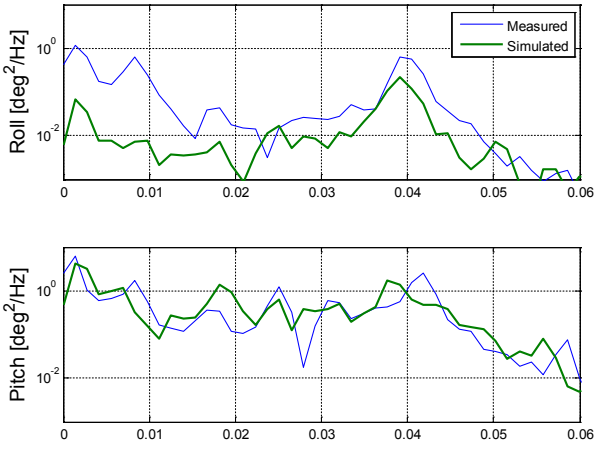

Fig. 11. Spectra of the rotational motions of the spar at low frequency for H_s = 1.4 m, T_p = 8.6 s.

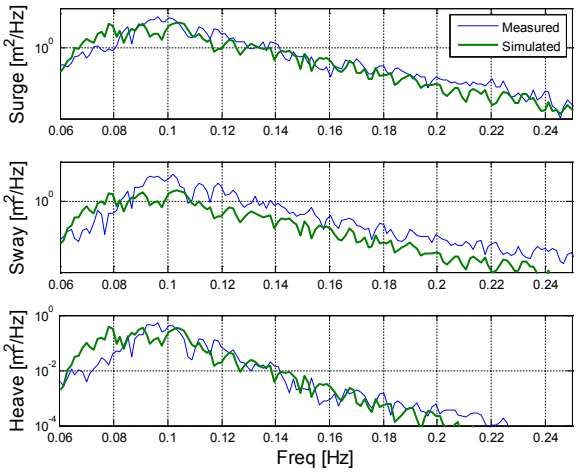

Fig. 12. Spectra of the translational motions of the spar in the wave-frequency range for H_s = 4.0 m, T_p = 10.0 s.

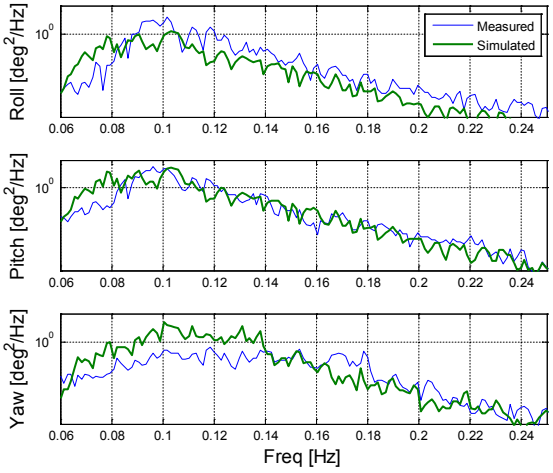

Fig. 13. Spectra of the rotational motions of the spar in the wave-frequency range for H_s = 4.0 m, T_p = 10.0 s.

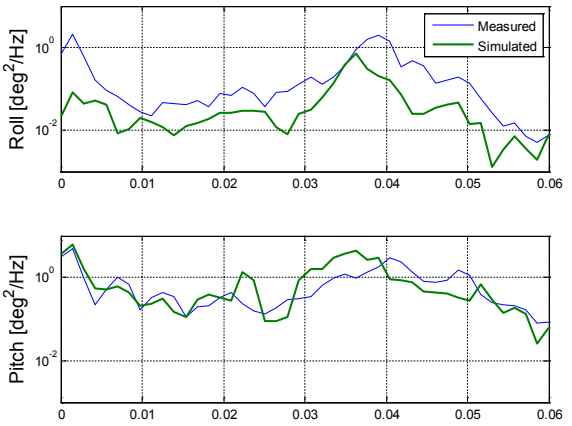

Fig. 14. Spectra of the rotational motions of the spar at low frequency for H_s = 4.0 m, T_p = 10.0 s.

6. Conclusions

As offshore wind development moves into deep water, the merit of a coupled computer model, such as FAST, for design is its ability to accurately predict the response of floating wind turbines under turbulent wind fields, irregular waves, and other environmental variables. Model validation against experimental data is critical to gain confidence that a model is accurate and able to adequately predict loads and motions of floating wind turbines. In this paper, we directly compared the measured response of Statoil's Hywind Demo spar offshore wind turbine with the predicted response from a representative FAST model exposed to similar wind and wave conditions.

After calibrating the mooring stiffness via small changes to the mooring line length and applying small scale factors to the mass distributions of the blades and tower, the model accurately predicted the natural periods of motion for the spar and the aggregate masses for the tower-top assembly and the turbine system. For both a fixed and floating structure, the model accurately produced the Siemens-supplied power curve, with some slight over-prediction in region 2, just below rated power.

By using the new TurbSim functionality to reproduce measured wind speed time series, and by using FAST to produce statistically similarly wave motions for environmental input, good agreement was found between the measured and simulated response. The model controller accurately reproduced the blade pitch and rotor speed over the range of wind speeds from 4 to nearly 24 m/s. Similarly, the predicted edge and flap blade-root moments agreed with the measured averages and variance. FAST slightly over-predicts the variance of the flap moment and under-predicts the average edge moment at higher wind speeds. The modeled and measured platform surge, sway, heave, roll, and pitch motions agree well over wave frequencies for both low (H_s = 1.4) and moderate (H_s = 4.0 m) seas. The roll response at low frequency and yaw response, however, does not agree well with the measured data. This is likely caused by both the application of a linear yaw stiffness instead of modeling the true nonlinear response of the mooring bridle attachment and to the real waves have spreading while they are modeled as unidirectional.

This validation effort presents a solid first step in assessing the accuracy of FAST for modelling the coupled response of a floating offshore wind turbine under realistic open-ocean conditions, which is critical to gain confidence that FAST is suitably accurate for application to developing innovative, optimized, reliable, and cost-effective floating offshore wind technology. Future work could involve: 1) improvement of the FAST blade and mooring models (by making use of the new BeamDyn and MoorDyn modules of FAST, respectively), 2) the direct use of measured wave time series, 3) quantification of measurement uncertainty and model sensitivity, and 4) analysis of additional cases, including parked/idling under extreme conditions.

Acknowledgements

The authors acknowledge the support of Siemens for providing the turbine data and walking us through the turbine configuration. This work was supported by the U.S. Department of Energy under Contract No. DE-AC36-08GO28308 with the National Renewable Energy Laboratory. Funding for the work was provided by the DOE Office of Energy Efficiency and Renewable Energy, Wind and Water Power Technologies Office.

References

[1] Damiani RR, Song H, Robertson AN, Jonkman JM. Assessing the Importance of Nonlinearities in the Development of a Substructure Model for the Wind Turbine CAE Tool FAST. Proceedings of the 34th International Conference on Ocean, Offshore and Arctic Engineering; 2014.

[2] Jonkman JM, Matha D. Dynamics of Offshore Floating Wind Turbines – Analysis of Three Concepts. Wind Energy; 2011; 14:557-569.

[3] Jonkman JM, Buhl ML. FAST User's Guide. NREL Technical Report NREL/EL-500-38230; 2005.

[4] Lee CH, Newman JN. WAMIT® User manual, Versions 6.3, 6.3PC, 6.3S, 6.3S-PC, WAMIT, Inc, 2006.

[5] Jonkman J, Larsen T, Hansen A, Nygaard T, Maus K, Karimirad M, Gao Z, Moan T, Fylling I. Offshore Code Comparison Collaboration within IEA Wind Task 23: Phase IV Results Regarding Floating Wind Turbine Modeling. European Wind Energy Conference (EWEC) 2010, 20-23 April, Warsaw, Poland.

[6] Robertson A, Jonkman J, Vorpahl F, Popko W, Qvist J, Froyd L, Chen X, Azcona J, Uzungoglu E, Guedes Soares C, Luan C, Yutong H, Pengcheng F, Yde A, Larsen T, Nichols J, Buils R, Lei L, Anders Nygard T, Manolas D, Heege A, Ringdalen Vatne S, Ormberg H, Duarte T, Godreau C, Fabricius Hansen H, Wedel Nielsen A, Riber H, Le Cunff C, Abele R, Beyer F, Yamaguchi A, Jin Jung K, Shin H, Shi W, Park H, Alves M, Guérinel M. Offshore Code Comparison Collaboration, Continuation within IEA Wind Task 30: Phase II Results Regarding a Floating Semisubmersible Wind System. 33rd International Conference on Ocean, Offshore and Arctic Engineering 2014, 8-13 June, San Francisco, California.

[7] Robertson A, Jonkman J, Masciola M, Molta P, Goupee A, Coulling A, Prowell I, Browning J. Summary of Conclusions and Recommendations Drawn from the DeepCWind Scaled Floating Offshore Wind. ASME 32nd International Conference on Ocean, Offshore and Arctic Engineering 2014, 9-14 June, Nantes, France.

[9] Koh JH, Robertson AN, Jonkman JM, Driscoll F, Ng EYK. Validation of SWAY Wind Turbine Response in FAST, with a Focus on the Influence of Tower Wind Loads. The Proceedings of the Twenty-Fifth International Ocean and Polar Engineering Conference 2015, 21-26 June, Kona, Hawaii; 1:538-546.

[9] Skaare B, Nielsen FG, Hanson TD, Yttervik R, Havmøller O, Rekdal A. Analysis of Measurements and Simulations From the Hywind Demo Floating Wind Turbine. Wind Engineering; 2013; doi: 10.1002/we.1750.

[10] Hanson TD, Skaare B, Yttervik R, Nielsen FG, Havmøller O. Comparison of measured and simulated responses at the first full scale floating wind turbine. EWEA 2011, Brussels.

[11] Skaare B, Hanson TD, Yttervik R, Nielsen FG. Dynamic Response and Control of the Hywind Demo Floating Wind Turbine. EWEA 2011.

[12] Bir GS. User's Guide to BModes (Software for Computer Rotating Beam Coupled Modes). NREL Technical Report NREL/TP-500-39133; 2007.

[13] Jonkman BJ. TurbSim User's Guide v2.00.00. NREL Technical Report, Draft Version 2014.